THE JOURNAL OF PHYSICAL CHEMISTRY A

Article

pubs.acs.org/JPCA

Strong Steric Hindrance Effect on Excited State Structural Dynamics of Cu(I) Diimine Complexes

Nosheen A. Gothard,[§,†] Michael W. Mara,[§,†,‡] Jier Huang,[‡] Jodi M. Szarko,[†,‡] Brian Rolczynski,[†,‡] Jenny V. Lockard,[‡,∥] and Lin X. Chen*[,†,‡]

[†]Department of Chemistry, Northwestern University, 2145 Sheridan Road, Evanston, Illinois 60208-3113, United States

[‡]Chemical Sciences and Engineering Division, Argonne National Laboratory, 9700 South Cass Avenue, Argonne, Illinois 60439, United States

Supporting Information

ABSTRACT: The metal-to-ligand-charge-transfer (MLCT) excited state of Cu(I) diimine complexes is known to undergo structural reorganization, transforming from a pseudotetrahedral D_{2d} symmetry in the ground state to a flattened D_2 symmetry in the MLCT state, which allows ligation with a solvent molecule, forming an exciplex intermediate. Therefore, the structural factors that influence the coordination geometry change and the solvent accessibility to the copper center in the MLCT state could be used to control the excited state properties. In this study, we investigated an extreme case of the steric hindrance caused by attaching bulky *tert*-butyl groups in bis(2,9-di-*tert*-butyl-1,10-phenanthroline)copper(I), $[Cu^I(dtbp)_2]^+$. The two bulky *tert*-butyl groups on the dtbp ligand lock the MLCT state into the pseudotetrahedral coordination geometry and completely block the solvent access to the copper center in the MLCT state of $[Cu^I(dtbp)_2]^+$. Using ultrafast transient absorption spectroscopy and time-resolved emission spectroscopy, we investigated the MLCT state property changes due to the steric hindrance and demonstrated that $[Cu^I(dtbp)_2]^+$ exhibited a long-lived emission but no subpicosecond component that was previously assigned as the flattening of the pseudotetrahedral coordination geometry. This suggests the retention of its pseudotetrahedral D_{2d} symmetry and the blockage of the solvent accessibility. We made a comparison between the excited state dynamics of $[Cu^I(dtbp)_2]^+$ with its mono-*tert*-butyl counterpart, bis(2-*tert*-butyl-1,10-phenanthroline)copper(I) $[Cu^I(tbp)_2]^+$. The subpicosecond component assigned to the flattening of the D_{2d} coordination geometry in the MLCT excited state was again present in the latter because the absence of a *tert*-butyl on the phenanthroline allows flattening to the pseudotetrahedral coordination geometry. Unlike the $[Cu^I(dtbp)_2]^+$, $[Cu^I(tbp)_2]^+$ exhibited no detectable emission at room temperature in solution. These results provide new insights into the manipulation of various excited state properties in Cu diimine complexes by certain key structural factors, enabling optimization of these systems for solar energy conversion applications.

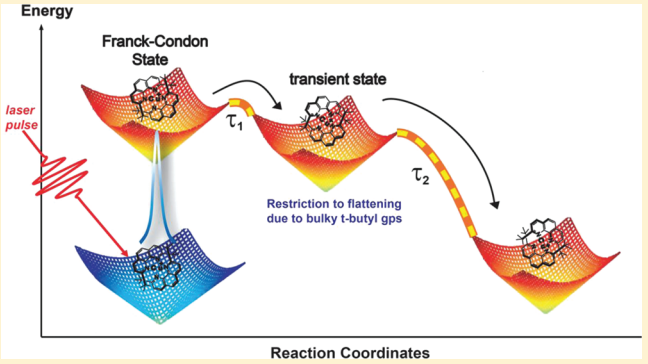

1. INTRODUCTION

The photoexcited states of transition metal complexes have important functions in solar energy conversion applications. In spite of their strong absorption in the visible spectrum and their ability to donate electrons in light-induced electron-transfer reactions, excited metal-to-ligand-charge-transfer (MLCT) states of Cu(I) diimine complexes have not been as readily utilized in light-driven fuel and electricity generation processes[1−11] as their Ru(II),[12−14] Os(II),[15] and Ir(III)[16] counterparts. This is in part due to lingering questions about their structural reorganization, strong solvent dependent excited state dynamics,[1,17] low oxidation potential,[18,19] and the lability of Cu(II) complexes[19] in the MLCT state. Without a broad and complete understanding of the structural factors that control their photoexcited dynamics, it will be difficult to successfully employ this family of complexes in solar energy applications. To that end, much effort has been focused on probing the correlation between structural factors and excited state dynamics of Cu(I) diimine complexes using transient optical and X-ray spectroscopies, enhancing our understanding of the structural factors that modulate the MLCT state properties of these complexes.

In Cu(I) bis-phenanthroline complexes, a subgroup of Cu(I) diimine complexes, placement of nonhydrogen groups at the 2,9 positions of the phenanthroline ligands has a profound structural influence on the MLCT state properties.[2,9,20−25] As shown in Scheme 1a, these Cu(I) complexes have a distorted tetrahedral D_{2d} geometry in the ground-state due to the Cu $3d^{10}$ configuration. Excitation in the visible region drives an MLCT transition that shifts electron density from the Cu(I)

Received: July 18, 2011
Revised: January 27, 2012
Published: January 31, 2012

   dx.doi.org/10.1021/jp211646p | *J. Phys. Chem. A* 2012, 116, 1984−1992

Scheme 1. (a) MLCT State Pathways for Cu(I) Diimine Complexes; (b) Investigated Complexes, Where the Sphere Represents a *tert*-Butyl Group

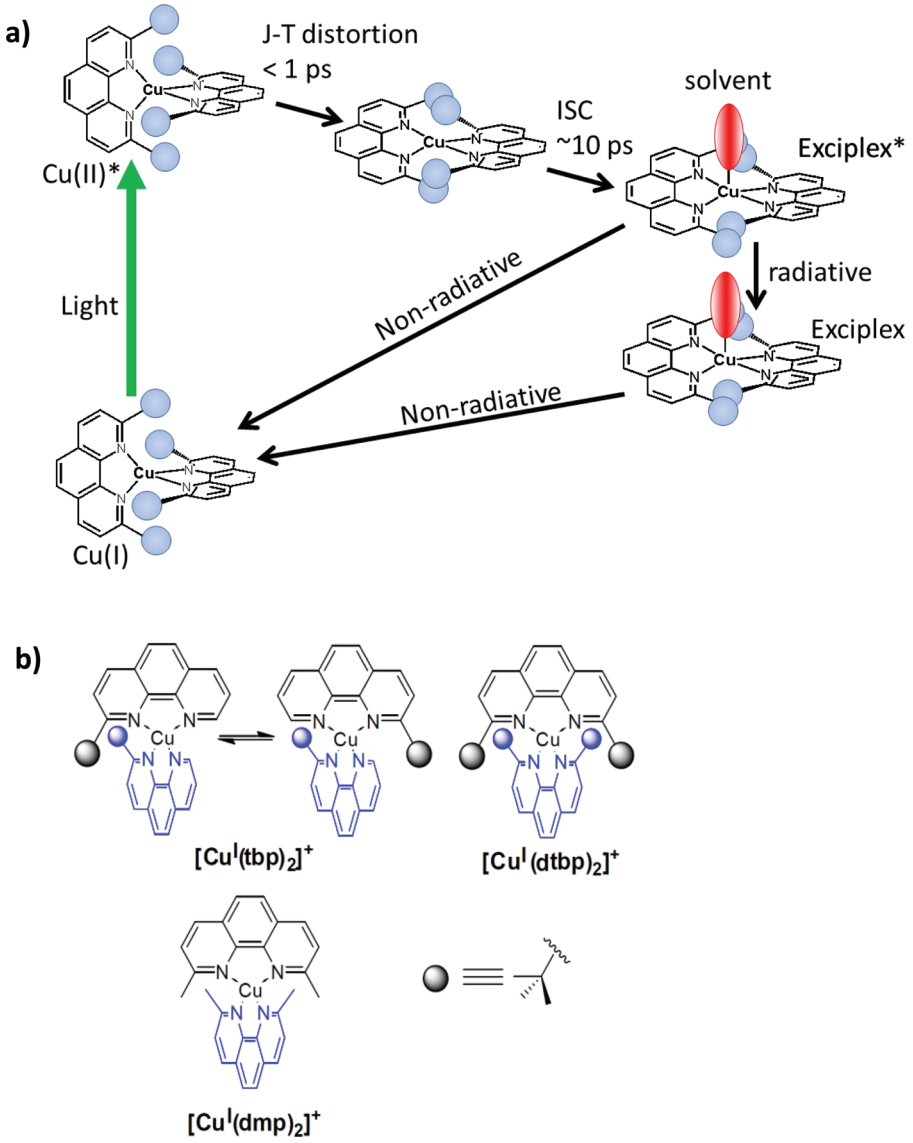

center to the ligands and transforms the Cu(I) center to nominally Cu(II) with a $3d^9$ configuration. Consequently, the asymmetric occupation of electrons in the 3d molecular orbitals (MOs) of the resulting Cu(II) center causes the Cu complex to undergo a Jahn–Teller distortion that transforms the ground state from a pseudotetrahedral coordination geometry with a D_{2d} symmetry to a flattened conformation with a D_2 symmetry in the thermally equilibrated MLCT state. The flattening opens one or two new coordination sites to which solvent molecules and other small ligands could bind, forming an exciplex-like structure with a reduced energy gap to the ground-state and, consequently, a shortened MLCT lifetime.[1,15] In our previous optical and X-ray transient absorption spectroscopic studies, an exciplex structure was identified for the MLCT state of bis(2,9-dimethyl-1,10-phenanthroline)copper(I), $[Cu^I(dmp)_2]^+$ in both coordinating and noncoordinating solvents.[26−29] The formation of this transient exciplex structure also opens a nonradiative decay pathway for the MLCT state quenching that is detrimental to solar energy conversion applications.[27,28] Nozaki and co-workers carried out studies on the MLCT state of $[Cu^I(dmp)_2]^+$ using quantum mechanical calculations and fluorescence lifetime measurements. They concluded that as the pseudotetrahedral coordination geometry flattens or the angle between the two ligand planes decreases, the MOs with strong spin–orbit (SO) coupling were destabilized, while the MOs with weak SO coupling were stabilized.[30] Because only those transitions to the latter were feasible, the thermally equilibrated flattened $[Cu^I(dmp)_2]^+$ MLCT state could have a much longer intersystem crossing (ISC) time than those of Ru(II) polypyridyl complexes[31,32] and hence >10 ps fluorescence lifetime.[30] Femtosecond transient absorption and fluorescence upconversion experiments[29,33] indicated that the Jahn–Teller distortion or the flattening time constant is <1 ps, and the other longer time excited state dynamics are dependent mainly on two structural factors, the angle between the two phenanthroline ligand planes and the solvent accessibility to the Cu center of the MLCT state. Hence, the MLCT state dynamics of this system could be controlled by tuning these two structural factors. More recently, the coherent movements of the MLCT state wavepackets have been observed through

dx.doi.org/10.1021/jp211646p | J. Phys. Chem. A 2012, 116, 1984−1992

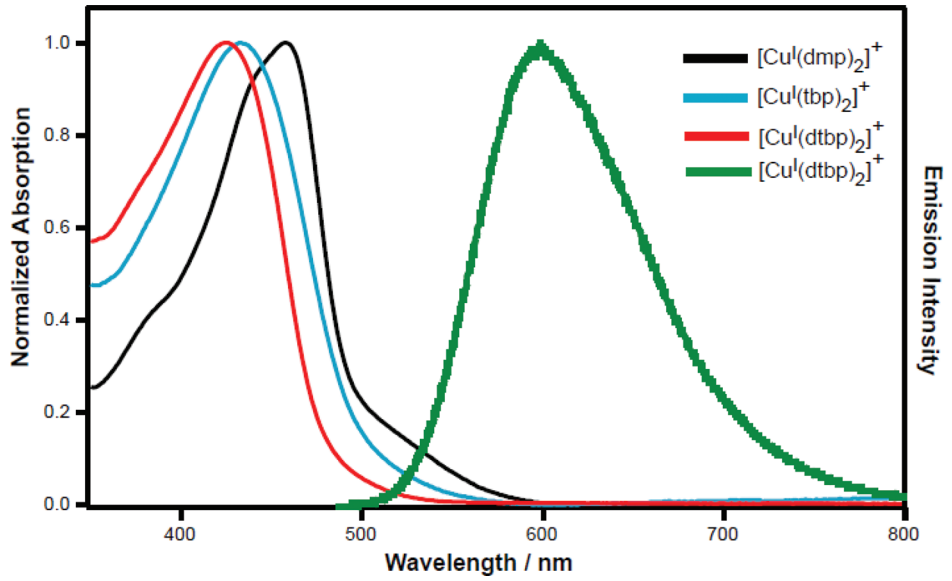

Figure 1. UV−vis absorption spectra of $[Cu^{I}(dtbp)_2]^+$ (red), $[Cu^{I}(tbp)_2]^+$ (blue), $[Cu^{I}(dmp)_2]^+$ (black), and steady-state emission spectra of $[Cu^{I}(dtbp)_2]^+$ (green) in dichloromethane with excitation at 400 nm.

ultrafast transient spectroscopy, shedding new light on the excited state transition from the initial Franck−Condon state to the thermally equilibrated MLCT state.[34]

One important question is whether the excited state properties can be controlled by restricting the distortion of the angle between the two ligand planes from the orthogonal to flattened conformation and thus limiting the solvent accessibility to the copper center. If we can understand the influence of structural factors on the excited state energetics and dynamic pathways, we will be able to systematically tune the ligand structures to ensure that the excited state properties of Cu(I) diimine complexes in terms of lifetimes and energies meet the requirements for solar energy conversion processes. In an attempt to answer the above question, we investigated the structural influence on the excited state dynamics in an extreme case of a completely locked tetrahedral coordinating geometry due to the sterically bulky *t*-butyl groups in bis(2,9-di-*tert*-butyl-1,10-phenanthroline)copper(I), $[Cu^{I}(dtbp)_2]^+$. In this report, we studied the behavior of the MLCT state of $[Cu^{I}(dtbp)_2]^+$, and those of its monosubstituted analogue bis(2-*tert*-butyl-1,10-phenanthroline)copper(I) $[Cu^{I}(tbp)_2]^+$, using ultrafast transient absorption and time-resolved emission spectroscopy. The influence of this extreme steric hindrance to the MLCT state reorganization and its implications in solar energy conversion will be discussed.

2. EXPERIMENTAL METHODS

2.1.1. Synthesis and Solution Sample Preparation. *$[Cu^{I}(tbp)_2]PF_6$.* The synthesis of $[Cu^{I}(tbp)_2]PF_6$ has been previously described.[35] The details have been presented in the Supporting Information.

2.1.2. $[Cu^{I}(dtbp)_2]SbF_6$. The synthesis of $[Cu^{I}(dtbp)_2]SbF_6$ has been previously described.[36] Please see Supporting Information for details.

Dichloromethane (Aldrich) solvent was distilled over calcium hydride for all spectroscopic measurements. Samples were made in a N_2-filled drybox. Approximately 1 mM solution samples were placed into a 2 mm path length freeze−pump−thaw cuvette under N_2 atmosphere for all optical experiments. Because water and coordinating solvents can replace the dtbp ligands in $[Cu^{I}(dtbp)_2]^+$ leading to sample decomposition, the samples were kept away from these substances during the entire experiment.

2.2. Steady-State Absorption and Emission Spectral Measurements. Ground state absorption spectra were acquired at room temperature using a Shimadzu UV-3600 UV−Vis-NIR spectrophotometer. The steady-state emission spectra were taken by an Ocean Optics dual grating spectrophotometer using 400 nm light excitation.

2.3. Ultrafast Transient Absorption(TA) Spectroscopic Measurements. TA measurements were performed with an apparatus based on an amplified Ti-Sapphire laser system (Spectra-Physics Mira Oscillator and Spitfire Pro Amplifier). The 415 nm excitation pulses were obtained from the second harmonic of the 830 nm amplifier output of the regenerative amplifier. A few micro-Joules of the fundamental output from the regenerative amplifier was focused onto a sapphire disk to generate the white light continuum and was split into two beams using a 50% beam splitter to yield the probe and reference pulses. The pump and probe beams were focused and spatially overlapped at the sample with a nearly collinear geometry and the relative polarization directions between the pump and probe pulses was set at the magic angle, 54.7°. The instrumental response function was ∼150 fs. The transient optical density changes at a particular probe wavelength λ, $\Delta OD(\lambda) = OD_{pump\text{-}on}(\lambda) - OD_{pump\text{-}off}(\lambda)$, as a function of the probe pulse delay time from the pump pulse, were analyzed by fitting the data with a multiexponential function convoluted with a Gaussian instrument response function.

2.4. Time-Correlated Single Photon Counting. Time-correlated single photon counting (TCSPC) measurements were taken using a setup from Ultrafast Systems (Halcyone). The 400 nm excitation pulses were generated by frequency doubling the 800 nm fundamental output of the Coherent RegA system. The excitation beam (∼10 nJ/pulse) was focused onto the sample, and the fluorescence signals were collected and passed through a long-pass filter. The emission signals were collected in the forward configuration and focused into a monochromator coupled with a photomultiplier tube (PMT).

The emission decays were measured using a Pendulum CNT-91 Timer/Counter/Analyzer. The fluorescence signals were collected at multiple wavelengths in the 500−650 nm region. The instrument response function for the TCSPC experiments was ∼150 ps fwhm. The emission signals were collected with a time interval of 50 ps/point, which were used directly to fit short time range kinetics in the nanosecond range, while binned raw data with 5 ns/point were used to fit kinetics in the microsecond range.

3. RESULTS

3.1. Steady-State UV−Vis Absorption Spectra. Steady-state UV−Vis absorption spectra of $[Cu^{I}(dtbp)_2]^+$, $[Cu^{I}(tbp)_2]^+$, and $[Cu^{I}(dmp)_2]^+$ in dichloromethane (Figure 1) have similar features in the 350−600 nm region with a main absorption peak maximized at 425, 432, and 454 nm, respectively. A shoulder feature on the red side of the absorption maximum has been assigned to low-lying MLCT transitions.[37−40] The main absorption peak position λ_{max} follows the order of $[Cu^{I}(dtbp)_2]^+$ < $[Cu^{I}(tbp)_2]^+$ < $[Cu^{I}(dmp)_2]^+$, while the steric hindrance for the Jahn−Teller distortion characterized by the angle between the two ligand planes follows a reverse order, indicating a reverse correlation between the steric hindrance and the energy of the lowest energy MLCT transitions. Because of the severe steric hindrance of the bulky *tert*-butyl groups at the 2,9 positions on the phenanthroline ligands, $[Cu^{I}(dtbp)_2]^+$ has a longer average Cu−N bond length (2.11 Å)[36,41] than the other Cu(I) diimine complexes (2.02−2.08 Å).[42−44] Consequently, the ground and MLCT states are destabilized, likely by different extents, the main MLCT band is blue-shifted, and the dtbp ligands in $[Cu^{I}(dtbp)_2]^+$ are more susceptible to ligand replacement reactions by coordinating solvents, such as water and acetonitrile.

As previously indicated, the lower-energy shoulder of the MLCT transition band of Cu(I) phenanthroline complexes is likely due to the dynamic flattening through low frequency rocking modes[45] of the presumed tetrahedral coordination geometry[46] with the D_{2d} symmetry, and its intensity increases as the probability of the complex to adopt a flattened geometry in the ground-state increases.[29,37,38] Relative to the $[Cu^{I}(dmp)_2]^+$ spectrum, where the shoulder feature is clearly visible around 525 nm, the $[Cu^{I}(dtbp)_2]^+$ spectrum has no shoulder feature at all because ∼100% of the ground-state population retains its D_{2d} symmetry in solution.

3.2. Transient Absorption Spectra and Kinetics of the $[Cu^{I}(dtbp)_2]^+$ MLCT State. Transient absorption spectra of $[Cu^{I}(dtbp)_2]^+$ in dichloromethane (Figure 2) were measured in the spectral region of 450−700 nm with 415 nm excitation. The negative absorption in the region of 450−480 nm is due to the ground state bleach (GB), while beyond 480 nm, the positive change in the absorbance is mainly due to the excited state absorption (EA). Initially a broad, featureless excited state absorption band arises >1 ps after excitation and later splits into three humps, presumably due to the vibronic features of the radical anion of the ligand typical of other Cu(I) phenanthrolines.[34,37] This radical formation also indicates the creation of the MLCT state immediately after excitation, where an electron density shift has taken place from Cu(I) toward the dtbp ligand(s). Once the humped features develop, their positions and shapes remain largely unchanged from 10 ps to 3 ns, unlike those seen for the less sterically constrained $[Cu^{I}(dmp)_2]^+$, where a continuous blue shift in the excited state absorption

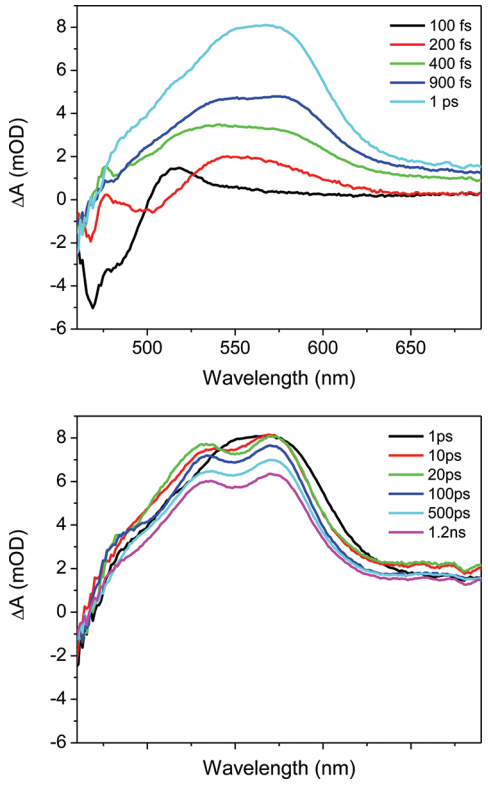

Figure 2. TA spectra of $[Cu^{I}(dtbp)_2]$ $[SbF_6]$ in dichloromethane from 100 fs to 1 ps (top) and 1 ps to 1.2 ns (bottom).

spectrum was observed during the first 20 ps after the excitation, which is normally attributed to vibrational cooling and triplet-state absorption due to ISC of the flattened MLCT state.

Kinetics traces for $[Cu^{I}(dtbp)_2]^+$ were collected in the spectral region from 540−610 nm in dichloromethane. The results of nonlinear least-squares fits of the data by multi-exponential functions are summarized in Table 1. The probe wavelengths were specifically monitored on the red side of the absorption band to observe the time scale of the spectral evolution from the initial broad spectrum to the transient spectrum with humped features. The time constants obtained from the fitting of the kinetics reveals two exponential decay constants: (a) a 4−10 ps time constant assigned to ISC and (b) a > 3 ns time constant assigned to the triplet ^{3}MLCT state decay to the ground state (Figure 4A,B). The absence of a subpicosecond rising component suggests that the Jahn−Teller distortion with the flattening motion seen in other Cu(I) diimine complexes is effectively blocked by the bulky *tert*-butyl groups at the 2,9 positions of the phenanthroline ligands. The absence of the blue shift indicates the absence of vibronic cooling because the bulky *tert*-bultyl groups completely shield the Cu center from solvent molecules.

Table 1. Excited State Kinetic Parameters of $[Cu^{I}(dtbp)_2]^+$ from TA Measurements; Samples Were Excited at 415 nm

probe wavelength (nm)	550	570	590	600	610
τ_1 (ps)	8.4		6.3	10.1	4.8
A_1 (%)	8		21	6	34
τ_2 (ps)	>3000	>3000	>3000	>3000	>6000
A_2 (%)	92	100	79	94	66

dx.doi.org/10.1021/jp211646p | J. Phys. Chem. A 2012, 116, 1984−1992

3.3. Transient Absorption Spectra and Kinetics of $[Cu^{I}(tbp)_2]^+$. The transient optical absorption spectra of the mono-*tert*-butyl substituted $[Cu^{I}(tbp)_2]^+$ in dichloromethane are displayed in Figure 3. The excited state absorption within 1

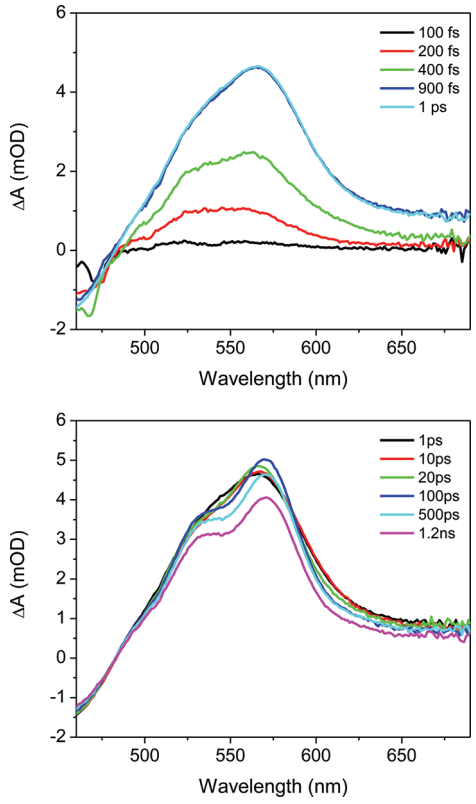

Figure 3. TA spectra of $[Cu^{I}(tbp)_2]$ $[PF_6]$ in dichloromethane from 100 fs to 1 ps (top) and 1 ps to 1.2 ns (bottom).

ps after excitation also appears to be broad and then evolves into a red-shifted, narrower spectrum with a dual peak structure (presumably due to vibronic features of the tbp radical anion) in ~100 ps. Kinetics for $[Cu^{I}(tbp)_2]^+$ in dichloromethane were also collected from 540–610 nm. The nonlinear least-squares fits of the kinetics data are listed in Table 2. The probe

Table 2. Excited State Kinetic Parameters of $[Cu^{I}(tbp)_2]^+$ from TA Measurements; Samples Were Excited at 415 nm

probe wavelength (nm)	550	570	590	600	610
τ_1 (ps)	0.23	0.26	0.43	0.45	0.59
A_1 (% rise)	100	89	83	78	100
τ_2 (ps)	9.3		13.1	17.9	10.3
A_2 (% rise)	6		42	60	33
τ_3 (ps)		61.2	68.2	44.2	
A_3 (% decay)		11	17	22	
τ_4 (ps)	>3000	>3000	>3000	>3000	>3000
A_4 (% decay)	94	69	58	40	67

wavelengths of $[Cu^{I}(tbp)_2]^+$ were monitored on the red side of the absorption band to provide the time scale of the spectral evolution from the initial broad spectrum to the narrowed, red-shifted transient spectrum.

Kinetics traces of $[Cu^{I}(tbp)_2]^+$ measured at different probe wavelengths are shown in Figure 4C,D. At all eight wavelengths, a subpicosecond rise component was observed, corresponding to the flattening process in other less sterically hindered Cu(I) diimine complexes.[29,33] It is important to note that this subpicosecond rise kinetics was not present in $[Cu^{I}(dtbp)_2]^+$ because this process has been blocked. $[Cu^{I}(tbp)_2]^+$ also exhibits a 50–60 ps rise in the EA signal only in the 580–590 nm region that was not observed in other Cu(I) diimine complexes. Although it is difficult to assign this rise component definitively at present, we suggest here a possible association of this rise component with the isomerization of the two different enantiomers of the tbp ligands as seen in Scheme 1b. Two additional decay components with time constants of 9–13 ps and >3 ns were extracted from the fitting. Judging by their values based on our previous studies, the faster time constant corresponds to ISC,[29] while the longer time constant is the triplet MLCT state lifetime with a time constant beyond the time window of the ultrafast TA measurements.

3.4. Time-Resolved Emission Measurements of $[Cu^{I}(dtbp)_2]^+$ by Time-Correlated Single Photon Counting (TCSPC). Time-resolved fluorescence measurements of the Cu(I) diimine complexes complement the transient absorption studies, providing information regarding the excited state decay pathways and ISC kinetics.[30] At least three groups have studied the fluorescence decay kinetics for the S_1 state of $[Cu^{I}(dmp)_2]^+$,[29,30,33] measuring short fluorescence lifetimes ranging from <100 fs to 20 ps. Unlike $[Cu^{I}(dmp)_2]^+$, which exhibits rather weak room temperature emission, $[Cu^{I}(dtbp)_2]^+$ in dichloromethane exhibits intense photoluminescence at room temperature with a quantum yield of 6%,[47] while no fluorescence on the time scale of less than a few picoseconds could be detected with the fluorescence upconversion method. Figure 5 shows the emission decay kinetics for $[Cu^{I}(dtbp)_2]^+$ in dichloromethane at 500, 600, and 650 nm, collected by TCSPC. According to the steady-state emission spectrum, the emission peaked at 599 nm with its blue edge onset at 500 nm (Figure 1). Therefore, our measurements cover from the blue to the red side of the steady-state emission band.

The emission decay dynamics are dependent on the probe wavelength with the decay time constants increasing at redder emission wavelengths (Figure 5). The results from the multiexponential fits are summarized in Table 3. The bluest emission at 500 nm was dominated by a component with a time constant less than the instrument response function and a minor component due to the fluorescence of the free ligands from the possible sample decomposition while the data were collected. At 600 nm emission, two longer emission lifetimes of 332 and 809 ns were detected with relative weights of 38% and 63%. The monoexponential decay at the emission wavelength of 650 nm reveals a 1.9 μs time constant corresponding to the lifetime of the ^{3}MLCT state, which is shorter than the 3.2 μs lifetime previously reported for this complex.[41] This may be due to an insufficient time window of 3 μs in our TCSPC measurements, which could yield the difference on the lifetimes. Nevertheless, the extremely long excited state lifetime and high photoluminescence yield agree with the previous results on the long time scale.[41]

In contrast, the mono-*tert*-butyl substituted $[Cu^{I}(tbp)_2]^+$ exhibits no room temperature luminescence even in a thoroughly degassed solution, which is likely due to the lack of a nonhydrogen substituent at the 9 position of the phenanthroline, leaving the Cu center at the MLCT state more susceptible to solvent ligation and subsequent quenching. Similar excited state behavior was also observed in other Cu(I)

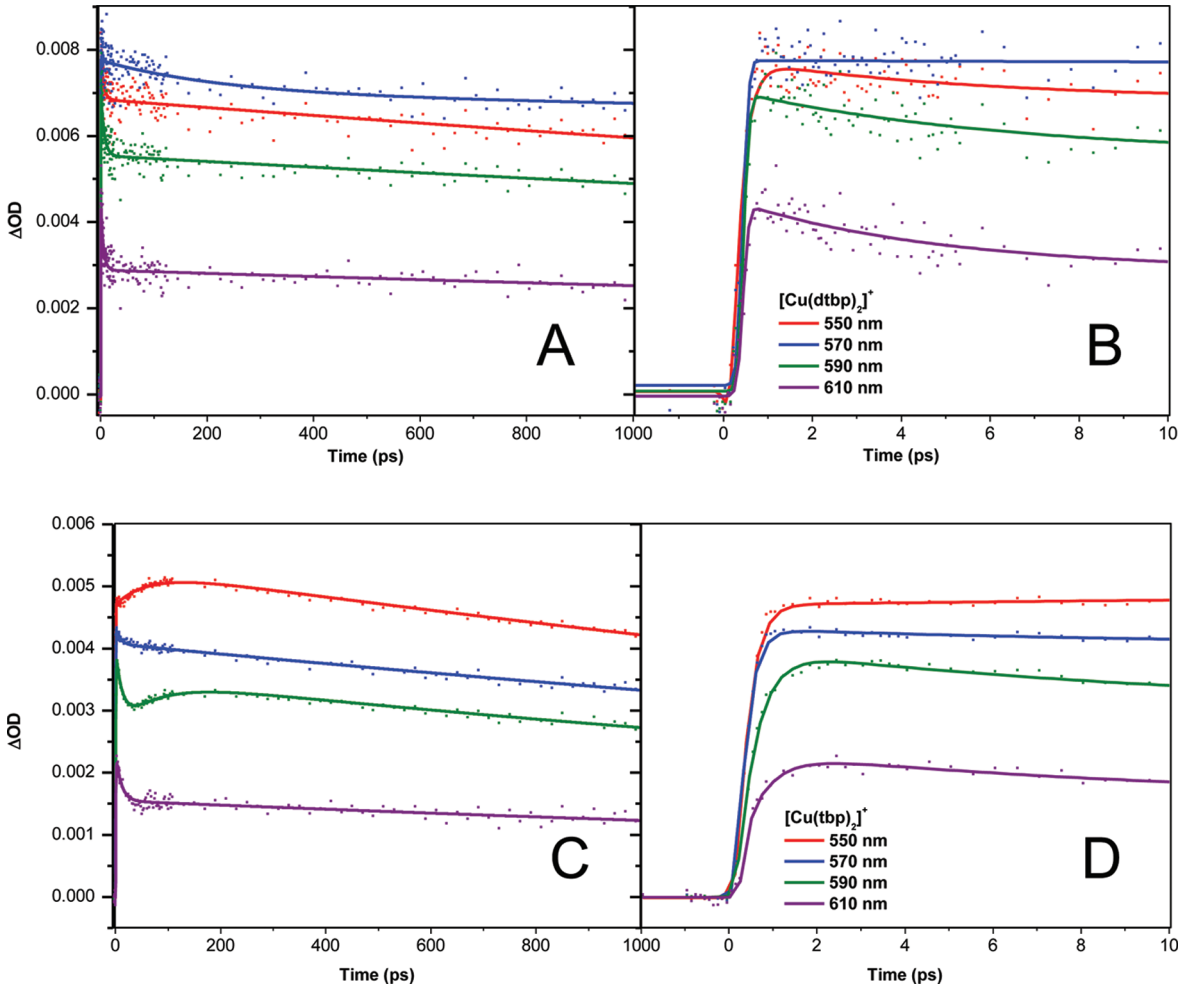

Figure 4. TA kinetics of $[Cu^{I}(dtbp)_2]^+$(A and B) and $[Cu^{I}(tbp)_2]^+$(C and D) at different probe wavelengths within 1 ns and 12 ps time windows. The excitation wavelength is 415 nm, and the probe wavelengths are as labeled.

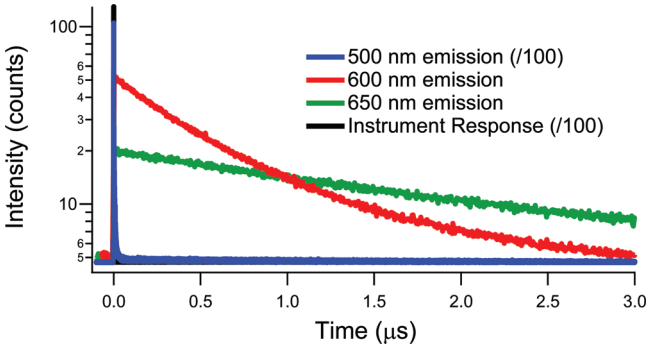

Figure 5. Fluorescence TCSPC decay kinetics of $[Cu^{I}(dtbp)_2]^+$ at different wavelengths with a 3 μs time window showing variation of the rate constants with emission wavelength. The excitation wavelength for the TCSPC experiment was 400 nm. Biexponential fits were used for the emission kinetics at 500 and 600 nm, while a monoexponential was used for 650 nm emission. The raw data were collected with 50 ps time intervals. The 600 and 650 nm emission curves are displayed by binned data with 5 ns intervals, where every 100 time points has been averaged. The instrument response is approximately 150 ps fwhm.

bis-phenanthroline complexes in dichloromethane with missing bulky groups at the 2 and 9 positions, even when the ligands have large groups at other positions.[26] As a result, transient absorption spectroscopy was left as the only means to ascertain the excited state dynamics of the $[Cu^{I}(tbp)_2]^+$ as described in section 3.3.

Table 3. Time Constants from Nonlinear Least-Squares Fitting of TCSPC Data at Various Wavelengths for $[Cu^{I}(dtbp)_2]^+$ in Dichloromethane; Sample Excited at 400 nm

emission wavelength (nm)	500	600	650
decay 1 (ns)[a]	0.15(95%)	332(38%)	
decay 2 (ns)[a]	3.5(5%)	809(62%)	1900(100%)

[a]The number in parentheses shows the normalized fractional amplitude for each component.

4. DISCUSSION

4.1. Effect of Structural Constraints on the Excited State Dynamics. Because $[Cu^{I}(dtbp)_2]^+$ provides an extreme case for severe structural constraints that inhibit the flattening due to the Jahn−Teller distortion and the solvent access to the copper center in the MLCT state (Scheme 1b), the excited state pathways and rate constants for individual steps (Scheme 1a from our previous studies on $[Cu^{I}(dmp)_2]^+$) need to be drastically revised. In order to analyze the influence of the structural constraint on the MLCT state dynamics, we will make a comparison of the potential surfaces of $[Cu^{I}(dtbp)_2]^+$

dx.doi.org/10.1021/jp211646p | J. Phys. Chem. A 2012, 116, 1984−1992

and $[Cu^{I}(dmp)_2]^+$ along one selected reaction coordinate, the angle between the two phenanthroline planes, φ, as shown in Figure 6. The potential surfaces are drawn based on both

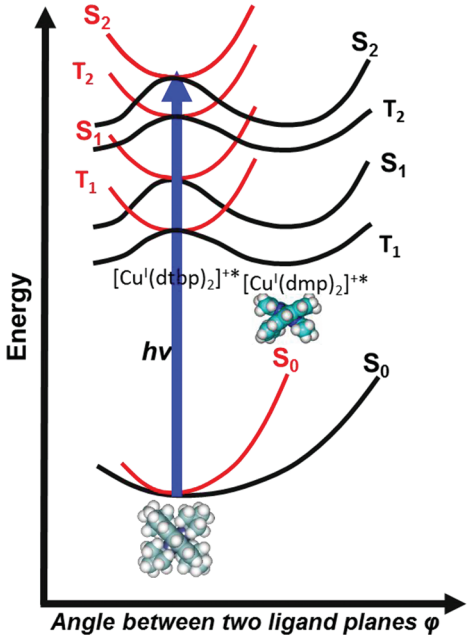

Figure 6. Potential energy vs the dihedral angle of the ligand orientations for Cu(I) phenanthroline complexes for the orthogonal geometry (left) and the flattened geometry (right). The excited state pathways are indicated by different arrows.

calculated results by Nozaki and co-workers[30] and the fluorescence upconversion and transient absorption results from our own studies as well as those from Tahara and co-workers.[29,33]

The first effect of the severe structural constraints on the MLCT state dynamics of $[Cu^{I}(dtbp)_2]^+$ is the disappearance of the subpicosecond component in the kinetics, which was observed in the MLCT state of $[Cu^{I}(dmp)_2]^+$ and assigned as the time constant of the flattening of the pseudotetrahedrdal coordination in the Franck–Condon state. Although a direct structural measurement on a femtosecond time scale with transient X-ray methods is not immediately feasible to prove this assignment, strong evidence from the fluorescence upconversion results support the assignment.[29,33] In our previous studies on $[Cu^{I}(dmp)_2]^+$, the prompt fluorescence observed at the bluest side of the emission spectrum, presumably from the pseudotetrahedral Franck–Condon state, was about 100 fs, while the fluorescence on the red side of the emission spectrum, presumably from the already flattened MLCT state, had a lifetime of >10 ps. These results can be nicely rationalized based on the MO energies and potential surfaces calculated by quantum mechanical calculations[30,45] as illustrated in Figure 6. On the basis of these calculations, a set of potential surfaces as a function of φ can be constructed for $[Cu^{I}(dmp)_2]^+$. When φ = 90° in the Franck–Condon state, the energy between S_1 and S_0 is larger than when φ decreases in the flattened geometry. The fact that the red emission with >10 ps in $[Cu^{I}(dmp)_2]^+$ could be observed suggested that the flattening must be on the subpicosecond time scale, comparable to the prompt fluorescence decay constant. Otherwise, there would be no more S_1 left because the subpicosecond prompted fluorescence decay at the Franck–Condon state would deplete nearly all population in the S_1 state. Tahara and co-workers obtained even more complete evidence on the subpicosecond structural reorganization due to the Jahn–Teller distortion through the entire transient fluorescence spectra.[33] The disappearance of this component in $[Cu^{I}(dtbp)_2]^+$ again confirms this assignment. Therefore, the nominally Cu(II) center at the MLCT state is forced into the less favorable pseudotetrahedral geometry without the fifth ligand. This situation is similar to copper sites in proteins with strong structural constraints around the metal sites as discussed extensively in the literature.[48,49]

The second effect on the MLCT state dynamics in $[Cu^{I}(dtbp)_2]^+$ is the intersystem crossing (ISC) time constant, τ_{ISC}. According to our previous results, τ_{ISC} for the MLCT state of $[Cu^{I}(dmp)_2]^+$ appeared to be φ dependent, ~100 fs when $\varphi \approx 90°$ in the Franck–Condon state and >10 ps when φ decreases (or flattens) since the energetically favorable orbitals exhibit weak spin–orbit coupling.[33] Therefore, with φ fixed at ~90° in $[Cu^{I}(dtbp)_2]^+$, one would expect to see a very short fluorescence decay time. However, we did not observe detectable subpicosecond fluorescence decay with the fluorescence upconversion method, in part due to sample integrity after long data acquisition time. We should emphasize that there could be a faster component beyond our detection capabilities by TCSPC with a 150 ps IRF.

The third effect on the MLCT state dynamics is the triplet lifetime. As flattening takes place in the MLCT state of $[Cu^{I}(dmp)_2]^+$, a solvent molecule ligates tightly or loosely with the copper center to form an exciplex, which lowers the energy of the MLCT state and enhances the nonradiative decay channel. Our previous X-ray transient absorption studies indicate that both coordinating and noncoordinating solvents form the exciplex with different interaction strengths and hence quench the excited state to different extents.[28] The triplet MLCT state lifetimes for $[Cu^{I}(dmp)_2]^+$ in strongly coordinating solvents are about 1–2 ns, while they are in the 100 ns range in weakly coordinating solvents. Therefore, one would expect that $[Cu^{I}(dtbp)_2]^+$ should have an MLCT state lifetime in the range of a few hundred ns. However, the measured $[Cu^{I}(dtbp)_2]^+$ photoluminescence lifetime is about a factor of 10 longer, ~1.9 μs at 650 nm. The MLCT state is long-lived because the copper center is completely shielded from the solvent–solute interactions in the MLCT state of $[Cu^{I}(dtbp)_2]^+$. Because acetonitrile or alcoholic solvents will replace the ligand in $[Cu^{I}(dtbp)_2]^+$, we were not able to measure the excited state dynamics in those strongly coordinating solvents. However, our previous results on the MLCT state of the Cu(I) bis-phenanthroline $[Cu^{I}(phen)_2]^+$ complex showed that the MLCT state lifetime was only a few ps when the copper center is completely exposed to solvent molecules even in a noncoordinating solvent, dichloromethane. These results together tell us that a complete shielding of the copper center from the solvent is the key to prolong the MLCT excited state lifetime.

Revised MLCT state dynamics for a severely constrained $[Cu^{I}(dtbp)_2]^+$ emerge as depicted by the red potential surface curves in Figure 6, showing the elimination of the flattening and solvent ligation shown in Scheme 1. Therefore, the complex will retain a D_{2d} symmetry throughout excited state pathways. However, we cannot rule out structural changes along other reaction coordinates, such as the Cu–N bond distances, but we were not able to determine the excited state structure due to the limited stability of the complex under the current X-ray

dx.doi.org/10.1021/jp211646p | J. Phys. Chem. A 2012, 116, 1984–1992

study conditions. The continuous evolution in the decay time constants of the photoluminescence at different emission wavelengths also suggests possibilities of other structural reorganization or inhomogeneity in the triplet state. However, we are not able to resolve these at present but will continue our investigation in the future.

The flattening of the MLCT state of $[Cu^{I}(tbp)_2]^+$ with only one *t*-butyl in the 9 position of the phenanthroline ligands is much less restricted than that of $[Cu^{I}(dtbp)_2]^+$ and appears to be more complicated due to the intrinsic chirality of the tbp ligand.[35] Even in the ground state, the monosubstituted Cu(I) complexes of this type are configurationally dynamic,[50] with a rapidly occurring equilibrium between the enantiomers in solution (Scheme 1b). The energy barrier for the exchange between the two enantiomers for $[Cu^{I}(tbp)_2]^+$ is 17.16 kcal·mol^{-1} according to our NMR measurements (see Supporting Information), and therefore, the flattening distortions of the MLCT state are not sufficiently blocked when the sole *tert*-butyl group is present on the phenanthroline. The subpicosecond rise of the MLCT excited state is similar to that of $[Cu^{I}(dmp)_2]^+$. The relaxation pathways for $[Cu^{I}(dmp)_2]^+$ and the two enantiomers of $[Cu^{I}(tbp)_2]^+$ are similar because the flattening and exciplex formation for $[Cu^{I}(tbp)_2]^+$ can occur when the *tert*-butyl groups yield from each other, allowing solvent molecules to enter the coordination sphere. Because of the missing substituent group at one of the two 2 or 9 positions of the phenanthroline ligands, certain conformations of this complex could allow solvent accessibility to the Cu in the MLCT state, similar to that in $[Cu^{I}(phen)_2]^+$ where the MLCT has a ps lifetime due to the exciplex formation, even in noncoordinating solvents such as dichloromethane.[26] This channel of solvent access may explain why $[Cu(tbp)_2]^+$ lacks room temperature emission. We also noticed that $[Cu(tbp)_2]^+$ was much more stable in solution, permitting us to collect data with better signal-to-noise for a prolonged period of time. This suggests a more stable Cu−N ligation when the steric hindrance is reduced.

4.2. Structural Requirements for Long-Lived MLCT States in Cu(I) Diimine Complexes. The role of the ground state geometry in the MLCT excited state lifetime is an ongoing discussion on whether the flattened or tetrahedral ground state coordination geometry will prolong the MLCT state lifetime of Cu(I) diimine complexes.[39,41] According to Nozaki and coworkers' calculations, $[Cu^{I}(dmp)_2]^+$ exhibits a slower ISC than Ru(II) polypyridyl complexes because the flattening distortions weaken SO coupling in this complex.[30] The energy gap between the ground state and the singlet and triplet states also varies with the angle φ between the two ligand planes (Figure 6). Our previous study predicted that the fluorescence lifetime varies from ∼100 fs to >10 ps as the φ changes from 90° to <70°.[29] The above statement focuses on the singlet MLCT state, while the long-lived and most commonly observed MLCT state in these complexes is the triplet MLCT state. The MLCT state dynamics of $[Cu^{I}(dmp)_2]^+$ showed that the subpicosecond and picosecond components corresponding to the flattening and ISC were inner sphere activities and largely solvent independent, whereas the nanosecond to longer components were solvent dependent. Therefore, the interplays between the structural constraints on inner and outer sphere activities involving both singlet and triplet MLCT states of these complexes need to be explored in the context of their functions for specific solar energy conversion applications.

One important aspect of this research involves determining the relationship between the structural factors and energy differences as well as the interconversion rates of the singlet, triplet, and ground states in this family of Cu(I) diimine complexes. Some less sterically hindered Cu phenanthrolines have already been extensively studied, such as $[Cu^{I}(phen)_2]^+$ and $[Cu^{I}(dmp)_2]^+$.[26,29,51,52] $[Cu^{I}(phen)_2]^+$ has an excited state lifetime of 1.5 ps; due to the lack of bulky substituents at the 2,9 positions of the phenanthroline, this complex is subject to quick exciplex quenching. In $[Cu^{I}(dmp)_2]^+$, however, the methyl groups at the 2,9 positions provide some protection against ligand attack to the Cu center, and therefore has a longer excited state lifetime of ∼100 ns in dichloromethane.[28] Since the methyl groups are relatively small compared to *tert*-butyl groups and thus only cause small van der Waals steric repulsions, this molecule experiences significant flattening distortions upon excitation, leading to a large singlet−triplet energy gap of 2950 cm^{-1}.[47] The bulky *tert*-butyl groups of $[Cu^{I}(dtbp)_2]^+$ prevent significant flattening, resulting in the much smaller singlet−triplet gap of 790 cm^{-1}.[47] Therefore, the singlet MLCT state of $[Cu^{I}(dtbp)_2]^+$ can be much shorter, and its triplet MLCT state can have higher energy than those complexes capable of flattening. The excited state deactivation pathways for these complexes are summarized in Figure 6. The singlet−triplet gap is smaller when flattening is blocked; thus, ISC is faster, while the gap is larger when the molecule flattens, extending the ISC lifetime. Thus, depending on the requirements for the specific applications, we can choose those complexes with longer singlet MLCT state lifetimes capable of flattening or those complexes with much longer triplet MLCT lifetimes with completely blocked flattening and solvent accessibility. On the basis of this study, the structural control factors for this group of Cu(I) complexes has become more clear, which will help in future applications.

Therefore, $[Cu^{I}(dtbp)_2]^+$ simultaneously possesses two distinct structural factors that prolong the MLCT state lifetimes, namely, (1) blocking the flattening distortions and (2) blocking the exciplex formation. Consequently, it has a very long ^{3}MLCT state lifetime. Because the excited state energy levels are relatively high, it could be able to function as the sensitizer dye in DSSCs if the stability can be improved through further chemical modifications.

5. CONCLUSIONS

The spectroscopic measurements of the two Cu(I) diimine complexes described in this work enhance our understanding of the correlation between steric hindrance from ligand substitution and excited state dynamics. The absence of a subpicosecond time component in the transient absorption kinetics of $[Cu^{I}(dtbp)_2]^+$ indicates the absence of flattening distortions. The increase in the ^{3}MLCT triplet state lifetime and quantum yield results from the shielding of the Cu center from solvent molecules, preventing exciplex formation. The rates of dynamic processes, such as internal conversion and ISC, are directly influenced by the size of substituents at 2,9 positions of the phenanthroline ligands. $[Cu^{I}(dtbp)_2]^+$ has a microsecond triplet-state lifetime that is longer than those of tris(bipyridyl)ruthenium(II), $[Ru^{II}(bpy)_3]^{+2}$, a complex commonly used in dye sensitized solar cells.[14,36,41] These results will help future modification of Cu(I) diimine complexes with energetic and long-lived excited states as well as high stabilities in different environments.

■ ASSOCIATED CONTENT

Supporting Information

Additional materials and characterization methods, ^{1}H NMR, ^{13}C NMR, synthesis schemes, and detailed procedures along with electrochemical measurements. This material is available free of charge via the Internet at http://pubs.acs.org.

■ AUTHOR INFORMATION

Corresponding Author

*Phone: 630-252-3533 or 847-491-3479. E-mail: lchen@anl.gov or l-chen@northwestern.edu.

Present Address

[‖]Department of Chemistry, Rutgers University-Newark, Newark, New Jersey 07102, United States.

Author Contributions

[§]These authors contributed equally to this work.

Notes

The authors declare no competing financial interest.

■ ACKNOWLEDGMENTS

We would like to acknowledge the supports by the U.S. Department of Energy, Office of Science, Basic Energy Sciences under Contract DE-AC02-06CH11357. We thank Professor SonBinh T. Nguyen for his advice in synthesis and characterization of the complexes as well as for hosting a part of the synthetic work in his laboratory at Northwestern University.

■ REFERENCES

(1) McMillin, D. R.; Kirchhoff, J. R.; Goodwin, K. V. *Coord. Chem. Rev.* **1985**, *64*, 83−92.
(2) Ruthkosky, M.; Kelly, C. A.; Castellano, F. N.; Meyer, G. J. *Coord. Chem. Rev.* **1998**, *171*, 309−322.
(3) Lavie-Combot, A.; Cantuel, M.; Leydet, Y.; Jonusauskas, G.; Bassani, D. M.; McClenaghan, N. D. *Coord. Chem. Rev.* **2008**, *252*, 2572−2584.
(4) Gray, H. B.; Maverick, A. W. *Science* **1981**, *214*, 1201−1205.
(5) Smith, C. S.; Mann, K. R. *Chem. Mater.* **2009**, *21*, 5042−5049.
(6) Benedict, J. B.; Coppens, P. *J. Am. Chem. Soc.* **2010**, *132*, 2938−2944.
(7) Bessho, T.; Constable, E. C.; Graetzel, M.; Redondo, A. H.; Housecroft, C. E.; Kylberg, W.; Nazeeruddin, M. K.; Neuburger, M.; Schaffner, S. *Chem. Commun.* **2008**, *32*, 3717−3719.
(8) Mutrofin, S.; Chan, E. J.; Healy, P. C.; Marinnelli, A.; Ngoune, J.; Pettinari, C.; Pettinari, R.; Somers, N.; Skelton, B. W.; White, A. H. *Inorg. Chim. Acta* **2008**, *361*, 2365−2374.
(9) Fry, H. C.; Lucas, H. R.; Sarjeant, A. A. N.; Karlin, K. D.; Meyer, G. J. *Inorg. Chem.* **2008**, *47*, 241−256.
(10) Lenzmann, F. O.; Kroon, J. M. *Adv. OptoElectron.* **2007**, 1−10.
(11) Nazeeruddin, M. K.; Grätzel, M. *Struct. Bonding* **2007**, *123*, 113−175.
(12) Paris, J. P.; Brandt, W. W. *J. Am. Chem. Soc.* **1959**, *81*, 5001−5002.
(13) Juris, A.; Balzani, V. *Coord. Chem. Rev.* **1988**, *84*, 85−277.
(14) Damrauer, N. H.; Cerullo, G.; Yeh, A.; Boussie, T. R.; Shank, C. V.; McCusker, J. K. *Science* **1997**, *275*, 54−57.
(15) Kober, E. M.; Caspar, J. V.; Lumpkin, R. S.; Meyer, T. J. *J. Phys. Chem.* **1986**, *90*, 3722−3734.
(16) Lowry, M. S.; Bernhard, S. *Chem.—Eur. J.* **2006**, *12*, 7970−7977.
(17) Kirchhoff, J.; McMillin, D.; Robinson, W.; Powell, D.; McKenzie, A.; Chen, S. *Inorg. Chem.* **1985**, *24*, 3928−3933.
(18) Patterson, G. S.; Holm, R. H. *Bioinorg. Chem.* **1975**, *4*, 257−275.
(19) Rorabacher, D. *Chem. Rev.* **2004**, *104*, 651−697.
(20) Ruthkosky, M.; Castellano, F. N.; Meyer, G. J. *Inorg. Chem.* **1996**, *35*, 6406−6412.
(21) Meyer, T. J. *Acc. Chem. Res.* **1989**, *22*, 163−170.
(22) Scaltrito, D. V.; Thompson, D. W.; O'Callaghan, J. A.; Meyer, G. *Coord. Chem. Rev.* **2000**, *208*, 243−266.
(23) Miller, M. T.; Gantzel, P. K.; Karpishin, T. B. *J. Am. Chem. Soc.* **1999**, *121*, 4292−4293.
(24) Miller, M. T.; Gantzel, P. K.; Karpishin, T. B. *Inorg. Chem.* **1999**, *38*, 3414−3422.
(25) Miller, M. T.; Karpishin, T. B. *Inorg. Chem.* **1999**, *38*, 5246−5249.
(26) Lockard, J. V.; Kabehie, S.; Zink, J. I.; Smolentsev, G.; Soldatov, A.; Chen, L. X. *J. Phys. Chem. B* **2010**, *114*, 14521−14527.
(27) Chen, L. X.; Jennings, G.; Liu, T.; Gosztola, D. J.; Hessler, J. P. *J. Am. Chem. Soc.* **2002**, *124*, 10861−10867.
(28) Chen, L. X.; Shaw, G. B.; Novozhilova, I.; Liu, T.; Jennings, G.; Attenkofer, K.; Meyer, G. J.; Coppens, P. *J. Am. Chem. Soc.* **2003**, *125*, 7022−7034.
(29) Shaw, G. B.; Grant, C. D.; Shirota, H.; Caster, E. W. Jr.; Meyer, G. J.; Chen, L. X. *J. Am. Chem. Soc.* **2007**, *129*, 2147−2160.
(30) Siddique, Z. A.; Yamamoto, Y.; Ohno, T.; Nozaki, K. *Inorg. Chem.* **2003**, *42*, 6366−6378.
(31) McCusker, J. K. *Acc. Chem. Res.* **2003**, *36*, 876−887.
(32) Bhasikuttan, A. C.; Suzuki, M.; Nakashima, S.; Okada, T. *J. Am. Chem. Soc.* **2002**, *124*, 8398−8405.
(33) Iwamura, M.; Takeuchi, S.; Tahara, T. *J. Am. Chem. Soc.* **2007**, *129*, 5248−5256.
(34) Iwamura, M.; Watanabe, H.; Ishii, K.; Takeuchi, S.; Tahara, T. *J. Am. Chem. Soc.* **2011**, *133*, 7728−7736.
(35) Hebbe-Viton, V.; Desvergnes, V.; Jodry, J. J.; Dietrich-Buchecker, C.; Sauvage, J.-P.; Lacour, J. *Dalton Trans.* **2006**, 2058−2065.
(36) Gandhi, B. A.; Green, O.; Burstyn, J. N. *Inorg. Chem.* **2007**, *46*, 3816−3825.
(37) Everly, R. M.; McMillin, D. R. *J. Phys. Chem.* **1991**, *95*, 9071−9075.
(38) Parker, W. L.; Crosby, G. A. *J. Phys. Chem.* **1989**, *93*, 5692−5696.
(39) Kalsani, V.; Schmittel, M. *Inorg. Chem.* **2006**, *45*, 2061−2067.
(40) Armaroli, N.; Accorsi, G.; Cardinali, F.; Listorti, A. *Top. Curr. Chem.* **2007**, *280*, 69−115.
(41) Green, O.; Gandhi, B. A.; Burstyn, J. N. *Inorg. Chem.* **2009**, *48*, 5704−5714.
(42) Hamalainen, R.; Ahlgren, M.; Turpeinen, U.; Raikas, T. *Crystal Struct. Commun.* **1979**, *8*, 75−80.
(43) Kovalevsky, A. Y.; Gembicky, M.; Novozhilova, I. V.; Coppens, P. *Inorg. Chem.* **2003**, *42*, 8794−8802.
(44) Miller, M. T.; Gantzel, P. K.; Karpishin, T. B. *Inorg. Chem.* **1998**, *37*, 2285−2290.
(45) Zgierski, M. Z. *J. Chem. Phys.* **2003**, *118*, 4045−4051.
(46) Cunningham, C. T.; Cunningham, K. L. H.; Michalec, J. F.; McMillin, D. R. *Inorg. Chem.* **1999**, *38*, 4388−4392.
(47) Asano, M. S.; Tomiduka, K.; Sekizawa, K.; Yamashita, K.-I.; Sugiura, K.-I. *Chem. Lett.* **2010**, *39*, 376−379.
(48) Solomon, E.; Sundaram, U.; Machonkin, T. *Chem. Rev* **1996**, *96*, 2563−2606.
(49) Holm, R.; Kennepohl, P.; Solomon, E. *Chem. Rev.* **1996**, *96*, 2239−2314.
(50) Meyer, M.; Albrecht-Gary, A. M.; Dietrich-Buchecker, C. O.; Sauvage, J. P. *Inorg. Chem.* **1999**, *38*, 2279−2314.
(51) Samia, A. C. S.; Cody, J.; Fahrni, C. J.; Burda, C. *J. Phys. Chem. B* **2004**, *108*, 563−569.
(52) Gunaratne, T.; Rodgers, M. A. J.; Felder, D.; Nierengarten, J.-F.; Accorsi, G.; Armaroli, N. *Chem. Commun.* **2003**, 3010−3011.